

Analysis of surface-plasmon-polaritons-assisted interference imaging by using silver film with rough surface

Sha Shi,^{1,2} Zhiyou Zhang,^{1,2} Mingyang He,^{1,2} Xupeng Li,^{1,2} Jing Yang,³ and Jinglei Du^{1,2,*}

¹Institute of Nanophotonics Technology, School of Physical Science and Technology, Sichuan University, Chengdu 610064, China

²Key Laboratory of High Energy Density Physics of Education Ministry, Sichuan University, Chengdu 610064, China

³Physical Engineering College, Zhengzhou University, Zhengzhou 45000, China

*dujl@scu.edu.cn

Abstract: In the surface plasmon polaritons (SPPs) interference lithography, the scattering effect caused by the rough surface of silver film deteriorates the quality of lithography patterns. Research shows that under this condition the light field in the photoresist is not the results of SPPs interference but comes from the SPPs assisted imaging in which the scattered light propagates from the upper surface of the silver film to the photoresist. The near-field optical transfer function (NOTF) is used to study this process and a method of evaluating the imaging quality is presented. The validity of NOTF is verified by both SPPs assisted interference imaging experiments and simulations by the FDTD. It is also shown that the NOTF method is not only a convenient approach to describe the nano-scale information transmission in the near-field but also a good method to optimize experimental parameters.

©2010 Optical Society of America

OCIS codes: (100.0100) Imaging process; (240.6680) Surface plasmons; (310.6628) Subwavelength structures, nanostructures.

References and links

1. X. Guo, J. Du, Y. Guo, and J. Yao, "Large-area surface-plasmon polariton interference lithography," *Opt. Lett.* **31**(17), 2613–2615 (2006).
2. Z. W. Liu, Q. H. Wei, and X. Zhang, "Surface plasmon interference nanolithography," *Nano Lett.* **5**(5), 957–961 (2005).
3. X. Luo, and T. Ishihara, "Surface plasmon resonant interference nanolithography technique," *Appl. Phys. Lett.* **84**(23), 4780–4782 (2004).
4. X. Luo, and T. Ishihara, "Subwavelength photolithography based on surface-plasmon polariton resonance," *Opt. Express* **12**(14), 3055–3065 (2004).
5. J.-Q. Wang, H.-M. Liang, S. Shi, and J.-L. Du, "Theoretical analysis of interference nanolithography of surface plasmon polaritons without match layer," *Chin. Phys. Lett.* **26**(8), 084208 (2009).
6. L. Fang, J.-L. Du, X.-W. Guo, J.-Q. Wang, Z.-Y. Zhang, X.-G. Luo, and C.-L. Du, "The theoretic analysis of maskless surface plasmon resonant interference lithography by prism coupling," *Chin. Phys. B* **17**(7), 2499–2503 (2008).
7. X. Guo, J. Du, X. Luo, C. Du, and Y. Guo, "Surface-plasmon polariton interference nanolithography based on end-fire coupling," *Microelectron. Eng.* **84**(5–8), 1037–1040 (2007).
8. H. Raether, *Surface Plasmons on Smooth and Rough Surfaces and on Gratings* (Springer-Verlag, 1988).
9. Z. Liu, S. Durant, H. Lee, Y. Pikus, Y. Xiong, C. Sun, and X. Zhang, "Experimental studies of far-field superlens for sub-diffractive optical imaging," *Opt. Express* **15**(11), 6947–6954 (2007).
10. Y. Xiong, Z. Liu, S. Durant, H. Lee, C. Sun, and X. Zhang, "Tuning the far-field superlens: from UV to visible," *Opt. Express* **15**(12), 7095–7102 (2007).
11. H. Lee, Z. Liu, Y. Xiong, C. Sun, and X. Zhang, "Development of optical hyperlens for imaging below the diffraction limit," *Opt. Express* **15**(24), 15886–15891 (2007).
12. S. Durant, Z. Liu, J. M. Steele, and X. Zhang, "Theory of the transmission properties of an optical far-field superlens for imaging beyond the diffraction limit," *J. Opt. Soc. Am. B* **23**(11), 2383–2392 (2006).
13. I. I. Smolyaninov, Y. J. Hung, and C. C. Davis, "Magnifying superlens in the visible frequency range," *Science* **315**(5819), 1699–1701 (2007).

14. V. A. Podolskiy, N. A. Kuhta, and G. W. Milton, "Optimizing the superlens: manipulating geometry to enhance the resolution," *Appl. Phys. Lett.* **87**(23), 231113 (2005).
15. H. Lee, Y. Xiong, N. Fang, W. Srituravanich, S. Durant, M. Ambati, C. Sun, and X. Zhang, "Realization of optical superlens imaging below the diffraction limit," *N. J. Phys.* **7**(1), 255 (2005).
16. P. G. Kik, S. A. Maier, and H. A. Atwater, "Image resolution of surface-plasmon-mediated near-field focusing with planar metal films in three dimensions using finite-linewidth dipole sources," *Phys. Rev. B* **69**(4), 045418 (2004).
17. V. G. Veselago, "The electrodynamics of substances with simultaneously negative values of ϵ and μ ," *Sov. Phys. Usp.* **10**(4), 509–514 (1968).
18. J. B. Pendry, "Negative refraction makes a perfect lens," *Phys. Rev. Lett.* **85**(18), 3966–3969 (2000).
19. J. B. Pendry, and S. A. Ramakrishna, "Near-field lenses in two dimensions," *J. Phys. Condens. Matter* **14**(36), 8463–8479 (2002).
20. N. Fang, H. Lee, C. Sun, and X. Zhang, "Sub-diffraction-limited optical imaging with a silver superlens," *Science* **308**(5721), 534–537 (2005).
21. D. O. S. Melville, R. J. Blaikie, and C. R. Wolf, "Submicron imaging with a planar silver lens," *Appl. Phys. Lett.* **84**(22), 4403–4405 (2004).
22. D. O. S. Melville, and R. J. Blaikie, "Super-resolution imaging through a planar silver layer," *Opt. Express* **13**(6), 2127–2134 (2005).
23. Z. Liu, H. Lee, Y. Xiong, C. Sun, and X. Zhang, "Far-field optical hyperlens magnifying sub-diffraction-limited objects," *Science* **315**(5819), 1686 (2007).
24. Z. Zhang, J. Du, X. Guo, X. Luo, and C. Du, "High-efficiency transmission of nanoscale information by surface plasmon polaritons from near field to far field," *J. Appl. Phys.* **102**(7), 074301 (2007).
25. Z.-Y. Zhang, J.-L. Du, Y.-K. Guo, X.-Y. Niu, M. Li, X.-G. Luo, and C.-L. Du, "Near-field optical transfer function for far-field super-resolution Imaging," *Chin. Phys. Lett.* **26**(1), 014211 (2009).
26. J. W. Goodman, *Introduction to Fourier Optics* (McGraw-Hill, 1968)
27. P. B. Johnson, and R. W. Christy, "Optical constants of the noble metals," *Phys. Rev. B* **6**(12), 4370–4379 (1972).
28. G. Qiu, and D. Cai, "Introduction to SPPs," *Physics Bimonthly* **28**(2), 472–494 (2006).

1. Introduction

In 2006, maskless SPPs interference lithography was presented based on the attenuated total reflection (ATR) coupling structure. This technique provides an appealing way to fabricate large-area nanostructures at low cost [1–7]. However, we find that the quality of lithography patterns is usually limited by the experimental technologies such as the controlling of the thickness of silver film and the degree of polarization of incident light; especially, how to control the roughness of the silver film surface is really a difficult problem to solve in real application. The rough surface of the silver film affects the propagation of light and deteriorates the quality of lithography patterns. Thus it is necessary to study this situation.

Usually people use optical transfer function (OTF) to describe the propagation of light in a linear imaging system. However, the propagation of light in the near field is so complicated that only in some specific situations the process could be described by OTF. In recent years, exciting progresses have been made in the developing of superlens [8–16]. Researches on superlens [17–23] indicate that a thin silver film can be used to realize super-resolution imaging, which means that the silver film could be treated as a linear imaging system in the near-field, so it is reasonable for us to introduce a general optical transfer function to study the near-field imaging with superlens. Recently NOTF is used to analyze the super-resolution imaging system with a thin silver film successfully [24,25]. The NOTF highlights the physical principles and simplifies the complicated numerical calculation. The calculation by using NOTF is much simple and timesaving than using the vector numerical calculation method.

In this paper, the SPPs interference lithography process is analyzed and discussed. It is found that when the surface of silver film is smooth it is a process of SPPs interference lithography and when there is small roughness on the surface it is an imaging process. Moreover, the characteristics of NOTF are investigated and a method of evaluating the near-field imaging quality of superlens is presented. Also the optimized experimental parameters for SPPs assisted interference imaging could be found by using NOTF and our experimental results agree with the calculations.

2. Near-field optical transfer function of silver superlens (NOTF_{Ag})

Figure 1 shows an interference imaging structure. In this structure the silver film contains a flat silver layer with thickness d and a rough scattering silver layer with (Root Mean Square) $\text{RMS} < 2.4\text{nm}$ according to our experiment. The silver film is surrounded by medium 1 and medium 3 whose dielectric constants are ϵ_1 and ϵ_3 , respectively. Two beams of coherent TM-polarized collimated monochromatic light form interference fringes in medium 1. If the surface of the silver film is smooth, the patterns in medium 3 are formed by the light which is attenuated by the silver film [as shown in Fig. 1(a)]. When the matching condition of surface plasmon resonance is satisfied the intensity of interference patterns in medium 3 is enhanced strongly, which has been discussed in [1]. If the surface is rough, scattered waves with different spatial frequencies transmit through the silver film and form the image in medium 3 [as shown in Figs. 1(b) and (c)]. For the evanescent waves are enhanced by the silver film, the image in medium 3 is formed with high resolution. Thus, the SPPs assisted interference imaging with a rough silver film is different from the SPPs interference lithography. In the following we will discuss the imaging process.

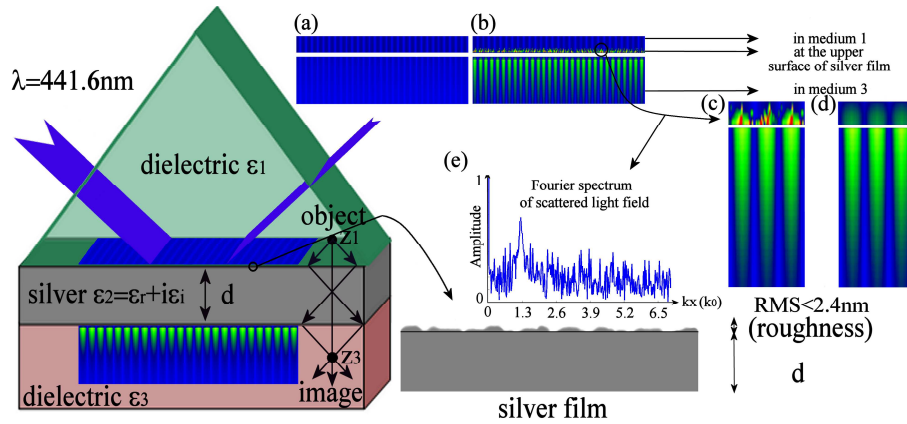


Fig. 1. Structure of imaging interference patterns with silver superlens. (a) Intensity distribution of light field when the surface of silver film is smooth. (b) and (c) Intensity distribution of light field when the surface is rough. (d) Intensity distribution of light field calculated with Eq. (2) and NOTF. (e) Fourier spectrum of the scattered light field at the upper surface of silver film, when the incident angle is 60° , wavelength of incident light is 441nm and $n_1 = 1.5$.

We can treat the rough surface of the silver film as a scatterer and the silver layer except the rough surface as a superlens [12]. Then the propagation of light and the imaging process can be described by a light field which is equivalent to the scattered light and a smooth silver layer which functions as a superlens, as shown in Fig. 1(d). The equivalent light field at the upper surface of silver film is described with the magnetic component $\vec{H}_o(\vec{r})$, which can be expressed as the Fourier integral over all the wave-vectors [26].

$$\vec{H}_o(\vec{r}) = \int \vec{H}_o(\vec{k}) \exp[i(\vec{k} \cdot \vec{r})] d\vec{k}. \quad (1)$$

In Eq. (1) $\vec{H}_o(\vec{k})$ is given by the Fourier expansion containing propagating and evanescent components.

$$\vec{H}_o(\vec{k}) = F(C(\cos \frac{4n_1\pi \sin \theta}{\lambda} x + 1) \text{random}(x)). \quad (2)$$

In Eq. (2) C is a constant, $\cos(4n_1\pi \sin \theta x / \lambda) + 1$ describes the interference patterns in medium 1, θ is the incident angle and λ is the wavelength of the incident light. $\text{random}(x)$

is a normalized random function which simulates the random scattering effect to the light and is determined by the rough silver film surface and in this paper we choose it from 0.7 to 1.3. The Fourier spectrum $\tilde{H}_o(\vec{k})$ of the scattered waves is shown in Fig. 1(e). Suppose that the incident waves are in x-z plane, the dispersion equations in different medium can be written as Eq. (3):

$$k_{ix}^2 + k_{iz}^2 = \varepsilon_i \omega^2 / c^2. \quad (i = 1, 2, 3 \text{ denote the three medium}) \quad (3)$$

For the propagating components ($k_{ix}^2 \leq \varepsilon_i \omega^2 / c^2$), there is $k_{iz} = (\varepsilon_i \omega^2 / c^2 - k_{ix}^2)^{1/2}$ and for the evanescent components ($k_{ix}^2 \geq \varepsilon_i \omega^2 / c^2$), there is $k_{iz} = i(k_{ix}^2 - \varepsilon_i \omega^2 / c^2)^{1/2}$. For each vector component, the transmission coefficient of the Fourier spectrum can be written as Eq. (4):

$$T = \frac{4\varepsilon_2\varepsilon_3k_{1z}k_{2z}\exp(ik_{2z}d)}{(\varepsilon_2k_{1z} + \varepsilon_1k_{2z})(\varepsilon_3k_{2z} + \varepsilon_2k_{3z}) + (\varepsilon_2k_{1z} - \varepsilon_1k_{2z})(\varepsilon_3k_{2z} - \varepsilon_2k_{3z})\exp(2ik_{2z}d)}, \quad (4)$$

where ε_2 is the permittivity of the metal. The dispersion equation of the silver film with finite thickness is written as Eq. (5):

$$(\varepsilon_2k_{z1} + \varepsilon_1k_{z2})(\varepsilon_3k_{2z} + \varepsilon_2k_{3z}) + (\varepsilon_2k_{z1} - \varepsilon_1k_{z2})(\varepsilon_3k_{2z} - \varepsilon_2k_{3z})\exp(2ik_{2z}d) = 0. \quad (5)$$

Below the silver film, the Fourier spectrum of the image is written as Eq. (6):

$$\tilde{H}_i = \tilde{H}_o(k_x)\exp(i \cdot z_1\sqrt{k_1^2 - k_x^2}) \cdot T \cdot \exp(i \cdot z_2\sqrt{k_3^2 - k_x^2}), \quad (6)$$

where z_1 is the distance from the object to the upper surface of the silver film (not including the roughness) and z_2 is the distance from the lower surface of silver film to the image. The image in the spatial domain is written as Eq. (7):

$$\vec{H}_i(\vec{r}) = \int \tilde{H}_i(\vec{k})\exp[i(\vec{k} \cdot \vec{r})]d\vec{k}. \quad (7)$$

The general NOTF of silver film is defined as \tilde{H}_i/\tilde{H}_o , so the $NOTF_{Ag}$ is written as Eq. (8):

$$NOTF_{Ag} = \frac{\tilde{H}_i}{\tilde{H}_o} = \exp(i \cdot z_1\sqrt{k_1^2 - k_x^2}) \cdot T \cdot \exp(i \cdot z_2\sqrt{k_3^2 - k_x^2}). \quad (8)$$

Figures 1(c) and 1(d) are gotten by FDTD method and NOTF method respectively, which shows that the results gotten by the two methods are much the same.

3. $NOTF_{Ag}$'s characteristics in different condition

It can be found from Eq. (8) that the $NOTF_{Ag}$ is closely related to the thickness of silver film, surrounding materials and transmission distance. In the calculations, the wavelength of the incident light is 441.6nm and the permittivity of silver is $\varepsilon_2 = -6.5 + 0.19i$ at this wavelength [27]. Figure 2(a) shows the curves of $NOTF_{Ag}$ of silver film with different thickness and fixed surrounding dielectric permittivity $\varepsilon_1 = \varepsilon_3 = 1.5^2$ (where $z_1 = 5\text{nm}$, $z_2 = 10\text{nm}$). It is clear that the propagating waves are always attenuated by the silver film. When the silver film is thin, the attenuated propagating waves can pass through; and when the silver film is thicker than 90nm, these waves becomes very weak. Besides, it should be noticed that when the silver film is thin, there are two peaks in the curves due to the split of degenerate state of surface plasmon resonance mode which is induced by the coupling between the surface plasmon resonances at both sides of the silver film. The two peaks correspond to the two resonant modes, respectively. As the thickness of the silver film increases, the first peak shifts to the right and the second peak shifts to the left which leads to the distance between them decrease simultaneously. At the same time, the first peak becomes lower and the second peak becomes narrower and higher. When d is larger than 90nm, the second peak disappears and the curve turns into the case of infinite thickness.

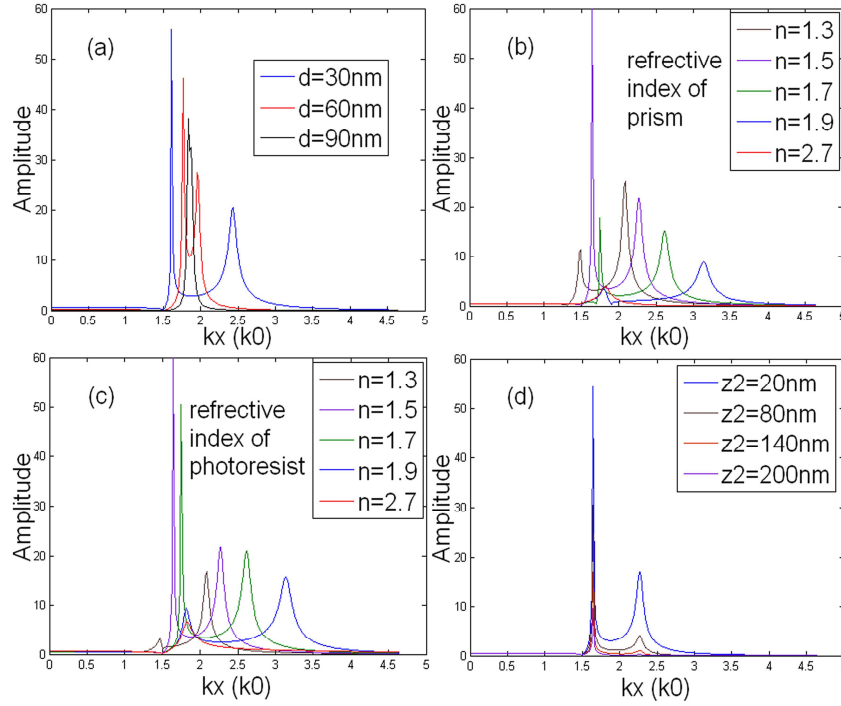


Fig. 2. Transfer functions of silver film in different conditions. (a) The curves of $NOTF_{Ag}$ with different thickness and $n_1 = n_3 = 1.5$. (b) The curves of $NOTF_{Ag}$ with different n_1 , $d = 40\text{nm}$ and $n_3 = 1.5$. (c) The curves of $NOTF_{Ag}$ with different n_3 , $d = 40\text{nm}$ and $n_1 = 1.5$. (d) The curves of $NOTF_{Ag}$ with different z_2 (fixing $z_1 = 5\text{nm}$) in condition of $n_1 = n_3 = 1.5$.

Here, we will give a simple illustration that the k_x corresponding to the peaks of $NOTF_{Ag}$ is the vector of surface plasmon resonance k_{spp} . First, rewrite the dispersion equation Eq. (5) as Eq. (9) [28]:

$$Y^\pm = \frac{k'_{2z}}{\varepsilon_2} + \frac{1}{2} \left[\left(\frac{k'_{1z}}{\varepsilon_1} + \frac{k'_{3z}}{\varepsilon_3} \right) \coth(k'_{2z}d) \pm \sqrt{\left(\frac{k'_{1z}}{\varepsilon_1} + \frac{k'_{3z}}{\varepsilon_3} \right)^2 \coth^2(k'_{2z}d) - 4 \frac{k'_{1z}}{\varepsilon_1} \frac{k'_{3z}}{\varepsilon_3}} \right]. \quad (9)$$

Solving the differential equation $dY^\pm/dk_x = 0$, we can obtain the values of k_x at the extreme points. In this condition, an intense enhancement to the evanescent waves occurs, which has always been regarded as surface plasmon resonance, and the corresponding k_x is the wave-vectors of surface plasmon resonance denoted as k_{spp} . Therefore, the transmission characteristics of silver film can be easily understood through $NOTF_{Ag}$, whose peak value is corresponding to the enhancement coefficient of surface plasmon resonance and the corresponding k_x is the matching wave-vector of surface plasmon resonance.

Figure 2(b) shows the curves of $NOTF_{Ag}$ with different refractive index of medium 1 (n_1). The thickness of silver film is $d = 40\text{nm}$, the refractive index of medium 3 is $n_3 = 1.5$ and n_1 varies from 1.3 to 2.7. As n_1 increases, both the peaks shift to the right, the amplitude of the first peak increase at first and then decreases and the amplitude of the second peak decreases. At the same time, the second peak becomes broader. The curves of $NOTF_{Ag}$ with different n_3 are shown in Fig. 2(c). n_3 varies from 1.3 to 2.7, $d = 40\text{nm}$ and $n_1 = 1.5$. As n_3 increases, the intensity of both the peaks increases at first and then decreases. Figures 2(b) and 2(c) indicate

that there is an optimal resonance condition to make the resonance peak highest and only when $n_1 > 1.2 \cdot n_3$ using prism to excite surface plasmon resonance is available while the silver film is smooth. Figures 2(b) and 2(c) also show that only when the dielectric constants of both medium 1 and medium 3 are less than the absolute value of the real part of the permittivity of silver ($|\epsilon_r|$) the two resonant peaks exist. When any of the dielectric constants ϵ is larger than $|\epsilon_r|$, the second peak disappears and the surface plasmon resonance degenerate mode occurs. Figure 2(d) shows the curves of $NOTF_{Ag}$ with different z_2 (fixing $z_1 = 5\text{nm}$). It shows that when $z_2 > 200\text{nm}$ the enhancement effect disappears, which leads to the image disappear.

4. Optimizing the parameters of silver superlens by $NOTF_{Ag}$

In this section we will discuss the excitation of surface plasmon resonance and the imaging quality with silver film.

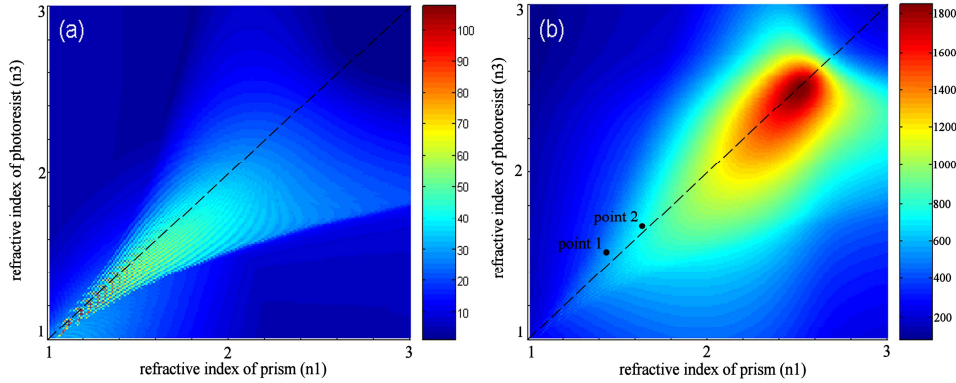


Fig. 3. (a) Intensity of the maximum peak of $NOTF_{Ag}$ varying with different medium 1 and 3, color bar denotes the enhancement of intensity. (b) Imaging quality with silver film varying with different medium 1 and 3, color bar denotes the total energy efficiency at the image surface.

Figure 3(a) shows the maximum peak value of $NOTF_{Ag}$ varying as n_1 and n_3 change ($d = 40\text{nm}$). We find that with given incident waves and silver film when both refractive indexes of medium 1 and medium 3 are low, the amplification of surface plasmon resonance is significant and any of them increasing will cause a weaker enhancement. The higher peaks locate slightly below the diagonal indicating that the strongest enhancement can be obtained only when n_3 is slightly smaller than n_1 in the structure with a finite thickness of silver film.

The SPPs assisted imaging by a silver superlens includes not only resonance wave-vector components but also other vector components as much as possible, thus the peak value of $NOTF_{Ag}$ cannot illustrate the imaging quality with silver film. So, we define the total energy efficiency at the image surface as the imaging quality evaluation function, which can be expressed as the integral of $NOTF_{Ag}$ over all the wave-vectors.

$$\eta = \int_{\text{all wave-vectors}} |NOTF_{Ag}|^2 dk_x. \quad (10)$$

Equation (10) is not normalized in order to indicate the enhancement effect of the silver superlens to evanescent waves. Usually for an imaging system there is a cut-off frequency and in this paper we define the spatial frequency at which the enhancement coefficient of evanescent wave is less than 1 as the cut-off frequency. Thus, Eq. (10) turns into a function with finite integrating range. Figure 3(b) shows the imaging quality with silver film. We notice that when ϵ_1 and ϵ_3 are getting closer to $|\epsilon_r|$ the imaging quality becomes better. And when $|\epsilon_2| = \epsilon_1 = \epsilon_3$, the imaging quality is the best, which agrees with the present theories and experimental results of silver super-resolution imaging [19–22].

5. Interference field transmission and imaging

Based on the analysis above, we calculate the SPPs assisted interference imaging with rough silver film by NOTF method and FDTD method. The calculating parameters are in the figure legends.

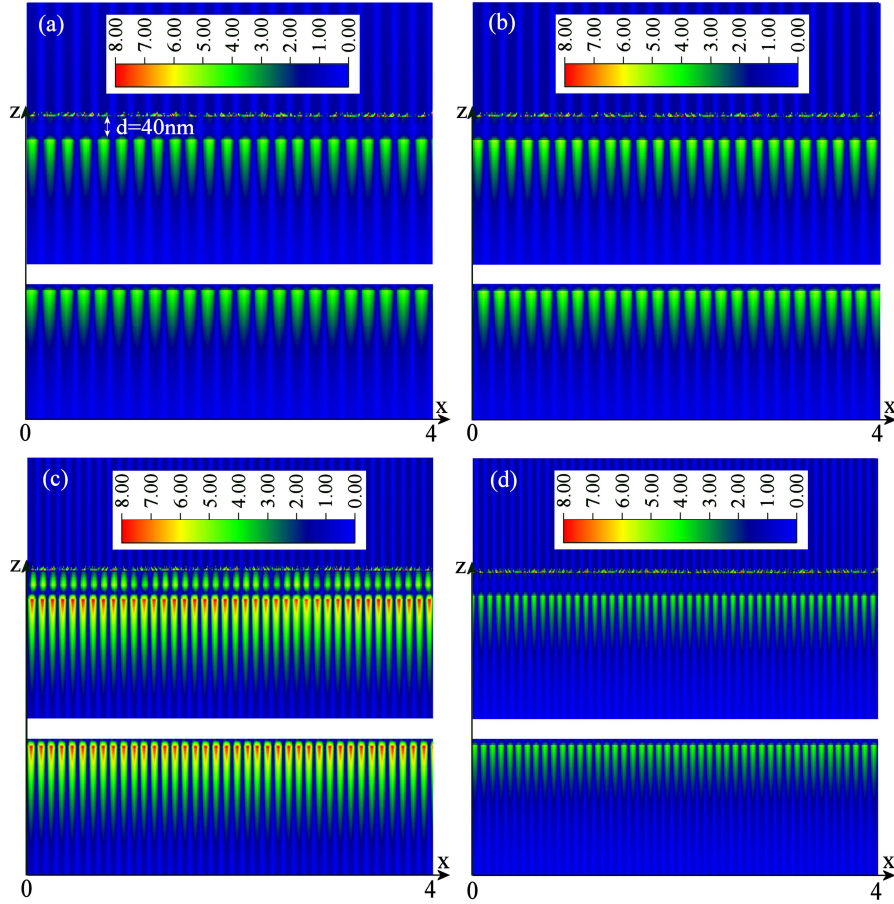


Fig. 4. The incident wavelength is 441.6nm and the incident angle is 60° . (a) The refractive indexes of dielectrics above and below the silver film are $n_1 = 1.47$ and $n_3 = 1.51$, respectively. (b) $n_1 = 1.61$ and $n_3 = 1.63$. (c) n_1 and n_3 are both 2.55. (d) $n_1 = 2.9$ and $n_3 = 2.9$.

The upper and lower figures in Figs. 4 (a) (b) (c) and (d) are based on the calculations by using FDTD and $NOTF_{Ag}$ methods respectively. We see that the $NOTF_{Ag}$ method gives us almost the same results as those given by FDTD method, but with a more uniformed distribution. The reason is that the quality of patterns obtained via FDTD is influenced by the length of steps, and the one obtained via $NOTF_{Ag}$ are not. The scattering effects caused by the rough layer are clearly shown in the Fig. 4 and do not damage the SPPs interference imaging. On the contrary they enhance the image quality. Figures 4(a) and 4(b) show the imaging process with $n_1 = 1.47$ and $n_3 = 1.51$ which corresponds to the Point 1 in Fig. 3(b) and the imaging process with $n_1 = 1.61$, $n_3 = 1.63$ which corresponds to Point 2, respectively. If the silver film is smooth, the matching conditions of surface plasmon resonance cannot be satisfied in these two cases and there will be no enhanced interference fringes in the medium 3 (it is not provided in this paper). But we can see in Fig. 4(a) and Fig. 4(b) that there is a distinct enhancement to the interference fringes and it should be attributed to the superlens imaging (our simulations demonstrate this point). The patterns in Fig. 4(b) are brighter than those in Fig. 4(a) since Point

2 is closer to the optimal imaging condition of the silver film than Point 1. Figure 4(c) shows the pattern imaged by silver film with $n_1 = n_3 = 2.55$ which satisfies the optimal imaging condition $|\varepsilon_2| = \varepsilon_1 = \varepsilon_3$. The evanescent components are enhanced most strongly which leads to the best quality of the image. We can see that there is a distinct image in the silver film in Fig. 4(c) which means that to TM-polarized waves a thin silver film can be regarded as LHM and the secondary imaging characteristic appears just when the permittivity of medium 1, medium 3 and silver are matched. In Fig. 4(d), $n_1 = 2.9$ and $n_3 = 2.9$. The imaging quality is relatively poor due to n_1 and n_3 deviating from the matching conditions. Figure 4 shows that when the matching condition $|\varepsilon_2| = \varepsilon_1 = \varepsilon_3$ is satisfied, the quality of the image is the best, which is consistent with the conclusion reached by using $NOTF_{Ag}$ method above. Besides the simulation results obtained from Fig. 4, we have also done lots of simulations with different $\varepsilon_1, \varepsilon_3$ ($1 < \varepsilon_1, \varepsilon_3 < 4$). And these results are consistent with the theory of $NOTF_{Ag}$. And for the SPPs assisted imaging, the quality of image has not much to do with the incident angle due to the scattering effects. Thus when the surface of the silver film is rough, the incident angle is no longer necessary to be the surface plasmon resonant angle, which promises the lithography patterns with a period of $\lambda/2n_1$.

In the experiment of Fig. 5(a), we chose prism (medium 1) with $n = 1.47$ and photoresist (medium 3) with $n = 1.51$, which was made by adding a small amount of resist-diluents in the AR-3170 ($n = 1.63$). In the experiment of Fig. 5(b), we chose prism with $n = 1.61$ and photoresist AR-3170. The parameters in Figs. 5(a) and 5(b) correspond to Point 1 and Point 2 in Fig. 3(b) respectively. Figure 5(a) is the imaging pattern with period of 173nm in the photoresist. In this experiment, the intensity of light in the photoresist is weak, which leads to the low-definition imaging pattern. In the experiment of Fig. 5(b) the pattern's period is 158nm. More amplified waves participate in the imaging process and the imaging quality is improved. The experimental results shown in Figs. 5(a) and 5(b) are consistent with the theory and simulations shown in Fig. 3(b), Figs. 4(a), and 4(b). Besides, the experimental results indicate that when the surface of silver film is rough the prism with a low refraction can be used to excite SPPs for imaging. With the same experimental condition mentioned above but the silver film is smooth we do not observe the surface plasmon resonance phenomena at any incident angle and no interference fringes are recorded in the corresponding experiment.

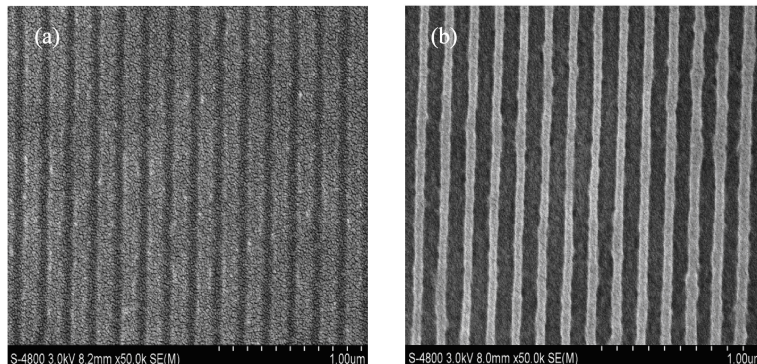


Fig. 5. Scanning electron microscope (SEM) image of the interference imaging in the photoresist with the incident wavelength 441.6nm and the incident angle 60°. (a) The refractive index of prism is 1.47 and the refractive index of diluted photoresist is 1.51. (b) The refractive index of prism is 1.61 and the refractive index of photoresist is 1.63.

6. Conclusion

In this paper, the SPPs assisted lithography by using a silver film with rough surface is regarded as an imaging process by a silver superlens. It is actually seeking an optimal matching condition

of dielectric constants of prism, photoresist and silver to generate better image. With $NOTF_{Ag}$, the simulation processes for providing experimental parameters of lithography and imaging are simplified and the optimal matching condition is found. With the SPPs assisted interference imaging, the quality of patterns in the photoresist could be well at different incident angles and the period is no longer single as that of the SPPs interference lithography. If the incident angle is not at the surface plasmon resonant angle the quality of the imaging patterns with a rough silver film is much better than that with a smooth silver film. And it should be noticed that if it is at the surface plasmon resonant angle the quality of lithography patterns with a smooth silver film surface is better than that with a rough silver film surface. The SPPs assisted interference imaging is researched experimentally, which is identical with the theory gotten by $NOTF_{Ag}$.

Acknowledgements

This work was supported by the National Basic Research Program of China under grant 2006CD302902 and the National Natural Science Foundation of China (NNSFC) under grant 60878031.